

## General Palaeontology (Taphonomy and Fossilization)

## Comparing rates of recrystallisation and the potential for preservation of biomolecules from the distribution of trace elements in fossil bones

Clive N. Trueman<sup>a,\*</sup>, Martin R. Palmer<sup>a</sup>, Judith Field<sup>b</sup>, Karen Privat<sup>b</sup>,  
Natalie Ludgate<sup>a</sup>, Valerie Chavagnac<sup>a</sup>, David A. Eberth<sup>c</sup>,  
Richard Cifelli<sup>d</sup>, Raymond R. Rogers<sup>e</sup>

<sup>a</sup> School of Ocean and Earth Science, University of Southampton, SO13 4ZH Southampton, UK

<sup>b</sup> Australian Key Centre for Microscopy and Microanalysis, University of Sydney, NSW 2006, Australia

<sup>c</sup> Royal Tyrrell Museum of Palaeontology, Drumheller, Alberta T0J 0Y0, Canada

<sup>d</sup> Geology Department, Macalester College, 1600, Grand Avenue, Saint Paul, 55015 Minnesota, USA

<sup>e</sup> Oklahoma Museum of Natural History, 2401, Chautauqua Avenue, Norman, 73072 Oklahoma, USA

Received 17 September 2007; accepted after revision 29 February 2008

Available online 22 April 2008

Written on invitation of the Editorial Board

---

**Abstract**

Preservation of intact macromolecules and geochemical signals in fossil bones is mainly controlled by the extent of *post-mortem* interaction between bones and sediment pore waters. Trace elements such as lanthanum are added to bone *post-mortem* from pore waters, and where uptake occurs via a simple process of diffusion and adsorption, the elemental distribution can be used to assess the relative extent of bone–pore water interaction and rate of recrystallisation. Distribution profiles can be parameterised effectively using simple exponential equations, and the extent of bone–water interaction compared within and between sites. In this study, the distribution of lanthanum within bone was determined by laser ablation ICP–MS in 60 archaeological and fossil bones from Pleistocene and Cretaceous sites. The rates of recrystallisation and potential for preservation of intact biogeochemical signals vary significantly within and between sites. Elemental profiles within fossil bones hold promise as a screening technique to prospect for intact biomolecules and as a taphonomic tool. **To cite this article:** C.N. Trueman *et al.*, C. R. Palevol 7 (2008).

© 2008 Published by Elsevier Masson SAS on behalf of l'Académie des sciences.

**Résumé**

**Comparaison des taux de recristallisation et du potentiel de conservation de biomolécules d'après la répartition d'éléments traces dans l'os fossile.** La conservation de macromolécules intactes ou de signaux d'éléments ou de leurs isotopes dans l'os fossile est contrôlée par l'étendue des interactions *postmortem* entre l'os et l'eau interstitielle dans la roche les contenant. Des éléments traces, comme le lanthane (La), sont ajoutés à l'os *postmortem* depuis les eaux interstitielles, et quand leur capture par l'os suit un simple processus de diffusion et d'adsorption, on peut utiliser la distribution de ces éléments pour évaluer l'importance des interactions entre l'os et l'eau interstitielle, relativement au taux de recristallisation. Des profils de répartition peuvent être effectivement paramétrés en utilisant de simples équations exponentielles et permettent de comparer l'importance des interactions os/eaux interstitielles dans un même site et entre sites. La répartition du lanthane dans l'os a été déterminée par ablation laser ICPM–MS dans 60 sites archéologiques et fossilifères, du Pléistocène et du Crétacé. Les taux de recristallisation et le potentiel pour la conservation de signaux

---

\* Corresponding author.

E-mail address: [trueman@noc.soton.ac.uk](mailto:trueman@noc.soton.ac.uk) (C.N. Trueman).

biogéochimiques intacts varient de façon significative entre sites et au sein d'un même site. Les profils élémentaires dans l'os fossile sont prometteurs en tant que technique d'échantillonnage pour évaluer la présence possible de biomolécules intactes et comme outil en taphonomie. **Pour citer cet article :** C.N. Trueman et al., C. R. Palevol 7 (2008).

© 2008 Published by Elsevier Masson SAS on behalf of l'Académie des sciences.

**Keywords:** REE; Diagenesis; Concentration gradient; Fossilization

**Mots clés :** REE (éléments terres rares) ; Diagenèse ; Gradient de concentration ; Fossilization

## 1. Introduction

One of the most startling developments in vertebrate palaeontology over the last decade has been the extraction, characterisation and sequencing of intact macromolecules from ancient bones [1,17,29,34]. The extent of molecular and geochemical preservation varies unpredictably between bones and depositional horizons [34,45] and as extracting biogeochemical information is destructive, expensive and time consuming, understanding the mechanisms leading to exceptional preservation is particularly important. Both molecular preservation and retention of biogenic geochemical signals depend upon a restricted degree of bone–water interaction during diagenesis. The duration of bone–pore water exchange is therefore a key variable which may have predictive power in identifying either conditions conducive to exceptional preservation or individual bones likely to yield molecular fossils. This study proposes a method to compare the relative duration of bone–pore water exchange between bones. Initially, however, we review the mechanisms by which bone mineral is preserved into deep time.

### 1.1. The nature of bone mineral

Bone mineral is composed of carbonated calcium phosphate minerals belonging to the apatite group. It has a range of lattice substitutions and a non-stoichiometric composition such that assigning bone mineral to a particular mineralogical form (e.g. dahllite) may lead to false impressions of homogeneity and well-ordered crystal chemistry. The size and shape of bone mineral crystallites is on the order of tens of nanometres in length and breadth, and 1–10 nm in thickness [12,33,47]. Bone crystallites are amongst the smallest of all biomineralised crystals, and their chemistry is dominated by their surface area/mass ratio and high degrees of lattice strain. The mineral component of bone is thermodynamically metastable and once exposed to pore-waters, bone crystallites will react, either dissolving or spontaneously recrystallising, increasing mean crystal sizes [2,26,43].

Bone mineral crystallites are intimately associated with the collagenous matrix in bone, essentially producing mineralised collagen fibrils. Bone crystallites are dispersed throughout the thickness of collagen fibrils oriented with their crystallographic 'c' axes aligned parallel to the direction of the collagen fibril [48]. The intimate association between crystal and protein shields crystallite surfaces from contact with pore fluids and also protects large organic molecules from enzyme attack [5]. Decomposition (hydrolysis) of collagen *post-mortem* exposes crystal surfaces and enhances dissolution, crystal reorganisation and recrystallisation of bone mineral [28,31,35,36,41]. Disruption of the crystal fabric in turn promotes enhanced diffusion of water and hastens the breakdown of the organic component [6,7]. In most burial environments, degradation of collagen and/or dissolution of bone mineral will therefore produce positive feedback leading eventually to dissolution and loss of the bone [28,31,35,36,41,43]. This process is dramatically enhanced by microbial activity, and most bones experiencing any form of microbial attack will not survive into deep time [15,40].

### 1.2. Fossilisation of bone

Fossil bones are almost universally composed of apatite crystals with larger crystal size and higher fluorine content than living bone and recrystallisation of bone apatite appears to be a requirement for preservation into deep time. Recrystallisation is a surface-driven process that is initiated by exposure of the crystallite surface through hydrolysis of collagen. Hydrolysis of collagen therefore promotes both the dissolution of apatite crystallites and their stabilisation and growth. Recrystallisation or growth of new apatite must occur relatively rapidly, as exposed crystallites would soon dissolve or be exploited biologically in most pore-water environments. It is likely that recrystallisation proceeds together with hydrolysis of collagen [3,5]; however, the relative rates of collagen loss and mineral growth are undoubtedly environment-specific, and are currently unknown.

In fossil bones the space left by collagen does not remain as pore space [16,41,53]. Fossil bones with no

surviving collagen, and composed exclusively of apatite group minerals, do not show pore spaces in regions originally occupied by collagen, clearly demonstrating authigenic growth of additional apatite *post-mortem* [17]. Hubert et al. [16] argued that diagenetic apatite was essentially added to biogenic ‘seed’ crystals. Where conditions allow, growth of seeded apatite continues until all inter-crystallite porosity has been infilled. In this model, fossilisation of bone is complete when growth of exposed apatite crystals closes the inter-crystalline porosity. Collagen fills ca. 25–36% of the volume of bone material *in vivo* [7,12], so in a fully recrystallised bone at least 25% of the volume must be composed of calcium phosphate that is entirely exogenous to the original bone ions. This exogenous or secondary calcium phosphate may be deposited within bone at any time *post-mortem* and will result in closure of the inter-crystalline porosity. Currently there are very few measurements of intra-crystalline porosity of fossil bones, however, increased mineral density is a ubiquitous feature of ‘fossil’ bones, and it is likely that closure of the intracrystalline porosity is a condition for survival of bone mineral into deep time, preventing continued interaction between sparingly soluble bone crystallites and pore waters.

The suggestion that bone fossilisation is accomplished largely by growth of additional (authigenic) calcium phosphate is supported by alteration of the stable isotope (particularly oxygen isotope) composition of bone during diagenesis. Oxygen is present in bone mineral in three main anions; phosphate, carbonate and hydroxyl. Oxygen-phosphorus bonds in phosphate are relatively strong and alteration of the isotopic composition of phosphate-bound oxygen during fossilization of bone must be accomplished either by substitution of phosphate ions at crystal surfaces or through growth of authigenic apatite. Several studies have attempted to demonstrate the extent of diagenetic alteration of phosphate-bound oxygen in fossil bone by exploiting the difference in isotopic composition of oxygen in freshwater and marine waters [27,42]. Typically such studies analyse the isotopic composition of articulated bones from exclusively terrestrial animals recovered from marine sediments. The articulated nature of the bones sampled ensures that carcasses were delivered to marine environments intact and did not experience prior burial in contact with terrestrial waters. The isotopic composition of phosphate oxygen in skeletons of terrestrial animals recovered from marine sediments is typically altered towards that of co-existing exclusively marine animals. In the study of Trueman et al. [42], the isotopic composition of marine and terrestrial animal bone recovered from marine sediments was indistinguishable

and clearly different from that of contemporaneous skeletons recovered from adjacent terrestrial sediments. As the pore space occupied by collagen accounts for only 30% of the volume of bone, the complete resetting of the phosphate-oxygen signal observed in this study requires growth of authigenic apatite, presumably in larger vascular canals such as canaliculi, osteocyte lacunae and haversian systems.

A major implication of this model is that continued *post-mortem* bone-pore water interaction is prevented by growth of authigenic apatite during early diagenesis. Isolation from continued interaction with pore waters is one mechanism that may lead to preservation of organic macromolecules provided the rates of recrystallisation are sufficiently rapid. Clearly, the relative rates of collagen hydrolysis, apatite crystal growth and closure of intra-crystallite porosity are crucial both to the long-term survival of bone and the potential preservation of labile macromolecules within bone. To understand the long-term preservation of biomolecules in ancient bone, it is therefore critical to assess the rates of recrystallisation of bone, and the environmental conditions that control these rates. The millennial timescales associated with recrystallisation of bone prevent realistic laboratory experimentation, but insights into the rates of recrystallisation of individual fossil bones may be gained by studying the *post-mortem* uptake of trace metals such as the rare earth elements (REE).

The total REE concentrations in bone *in vivo* are typically on the order of 1 part per million [41]. REE are ubiquitous in pore waters but present in low concentrations (on the order of parts per trillion). Bone crystallites have a high surface area and high cation exchange capacity. REE are thus readily sorbed onto bone crystal surfaces *post-mortem*, and while bone crystal surfaces are in contact with pore waters, their total REE content will increase [43]. The REE content of fossil bone has been used extensively as a proxy for ancient seawater chemistry [14,19,20,52], as a taphonomic tool to indicate and trace reworking [23,37,39,44] and as a palaeoenvironmental indicator [20,24,45,49,50]. Preservation of trace element and isotopic signals indicative of early burial environments indicates that later diagenetic conditions do not significantly alter the trace element composition, and thus that, once recrystallisation is complete, the fossil bone effectively acts as a closed system. The preservation of REE patterns in bone indicative of early depositional environments therefore provides a first estimate of  $10^4$ – $10^5$  years as the likely rate of recrystallisation in natural settings [22,41,45]. Further insights into the rates of recrystallisation of bone can be obtained by investigating the distributions of REE in fossil bones.

### 1.3. Concentration profiles of trace metals in ancient bone

The simplest mechanism by which elements are delivered to a porous material such as bone is via diffusion from surrounding pore waters through interconnected pore spaces [25]. During the initial, early phase of uptake, concentrations of any diagenetically added trace element will show steep gradients across the thickness of the bone, with highest concentrations at the bone margins. Continued diffusion will result in shallowing of concentration gradients and at equilibrium will lead to an even distribution of trace elements throughout the full thickness of the material [25,30]. A bone that remains in continual contact with pore fluids will therefore eventually reach equilibrium conditions where the concentration profile of any given element will be a flat line, the absolute concentration determined by the adsorption coefficient and concentration of that element (or elemental complex) in groundwaters. However, uptake of trace elements into bone *post-mortem* is coincident with recrystallisation of apatite and closure of intra-crystalline porosity. If uptake occurs though a simple single-event process of diffusion and adsorption, and closure of bone porosity occurs before the bone equilibrates with the surrounding pore waters, then a smooth concentration gradient will be preserved in the bone, the slope of the gradient controlled by the affinity of the element to bone apatite (the adsorption coefficient) and the extent of bone-pore water interaction. If the adsorption coefficient is sufficiently high, then bones may recrystallise before equilibration is reached. Many analyses of fossil bones have demonstrated concentration gradients in elements such as the REE and U [11,17,18,41] indicating that equilibration typically takes longer than the predicted  $10^4$ – $10^5$ -yr timescale of recrystallisation. The slope of the concentration gradients for these elements therefore gives an indication of the extent of interaction between bone and groundwater.

Bones are geometrically complex materials experiencing diagenesis in a range of dynamic hydrological conditions. Variations in bone geometry, the delivery of trace elements through bone, and the external concentrations of trace elements in surrounding groundwater may all influence the pattern of trace element uptake into bone. Several patterns of element distribution can be predicted reflecting contrasting uptake histories (Fig. 1):

- smooth concentration gradients, indicating diffusion of elements from surrounding groundwaters through interconnected water-saturated bone pore spaces and

removal of elements from solution via adsorption (Fig. 1A);

- flat profiles, indicating elemental equilibrium between bone crystal surfaces and external ground waters (Fig. 1A);
- oversteepened profiles, indicating either late diagenetic addition of trace elements at external margins (where further diffusion of trace elements into bone is

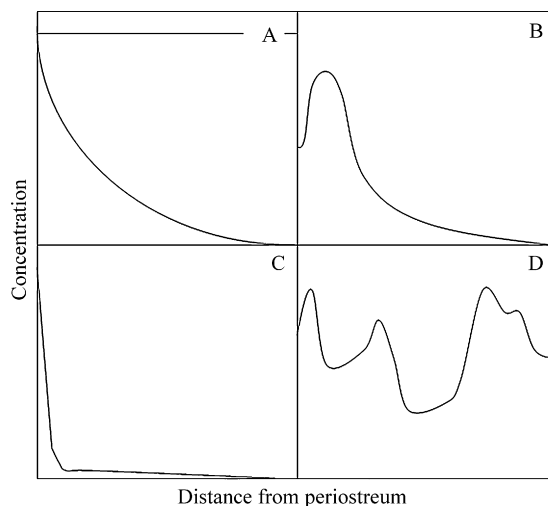


Fig. 1. Cartoon summarizing concentration profiles likely to be found in fossil bones (after Pike et al., [30]). (A) Concentration gradients consistent with uptake via simple single-phase diffusion adsorption mechanisms. Flat profile represents equilibrium between bone and pore waters. (B) Concentration gradient expected after leaching of trace elements from outer surfaces following a drop in external trace element concentrations. (C) Oversteepened concentration gradient consistent with either restricted contact between bone and pore waters via rapid recrystallisation or limited pore water exchange (in which case absolute concentrations in the internal surfaces will be similar to *in vivo* concentrations) or continued late diagenetic uptake of trace elements after recrystallisation (in which case internal concentrations will be significantly higher than *in vivo* concentrations). (D) Irregular concentration gradients, consistent with diffusion from multiple sources within vascularised bone.

Fig. 1. Schéma résumant les profils de concentration qu'il est vraisemblable d'observer dans les os fossiles (d'après Pike et al. [30]). (A) Gradients de concentration en accord avec un enrichissement selon un simple mécanisme d'adsorption/diffusion. Le profil plat représente l'équilibre entre l'os et les eaux interstitielles. (B) Gradients de concentration attendus après lessivage des éléments traces depuis les surfaces externes suivant une baisse de leur concentration externe. (C) Concentrations en « surpente » attendues, soit (1) d'un contact restreint entre l'os et les eaux interstitielles du fait d'une recrystallisation rapide, ou d'un échange limité avec les eaux interstitielles (dans ce cas, les concentrations absolues dans les surfaces internes seront semblables aux concentrations *in vivo*), soit (2) de la poursuite d'un enrichissement diagénétique tardif en éléments traces, après recrystallisation (dans ce cas, les concentrations internes seront significativement plus élevées que les concentrations *in vivo*). (D) Gradients de concentration irréguliers, en accord avec une diffusion à partir de sources multiples dans de l'os vasculaire.

limited by the lack of internal pore spaces) or extremely rapid recrystallisation of bone (Fig. 1C);

- M-shaped profiles, indicating leaching of trace elements from outer surfaces (Fig. 1B);
- irregular profiles, indicating complex non-diffusion–adsorption uptake and/or multiple phase uptake/leaching processes (Fig. 1D).

In this study, we investigate the potential of using trace element concentration profiles as a measure of the extent of interaction between bone and pore waters and the rate of recrystallisation of bones.

## 2. Materials and methods

A list of the samples is provided in Table 1.

### 2.1. Cuddie Springs

Twenty bone samples were obtained from stratigraphic units 6–9 of the archaeological site of Cuddie Springs in north-central NSW, Australia [13,44]. The sedimentary sequence at Cuddie Springs consists of at least 10 m of stratified, bone-bearing sediments, deposited in a lacustrine or clay-pan environment. The lowest sampled stratigraphic unit (SU9) is dated at >36 ka and is a condensed horizon within more than a meter of fine-grained, locally laminated, lacustrine sediments. SU9 contains abundant articulated and disarticulated remains of extinct and extant taxa. Stratigraphic unit 7 (SU7) comprises ferruginised sands overlain by a coarse, compacted conglomerate within a silty clay matrix that may reflect local flooding following a pluvial event. Stratigraphic unit 6 (SU6) is dated between ~30 and 36 ka, reflects a return to low energy conditions and contains two distinct stratigraphic units – SU6A and SU6B. SU6B (~36 ka) is comprised of manganese-coated peds, which together with the palynological evidence, indicates extended lake full conditions. The state of preservation of bones from Cuddie Springs varies from completely recrystallised to soft and unrecrystallised. Bones from the lowest levels are all strongly recrystallised, whereas bones from the upper layers display varying levels of recrystallisation. Bones from Cuddie Springs contain very low organic contents and do not yield sufficient collagen for  $^{14}\text{C}$  dating [8]. A detailed discussion of the nature of bones from Cuddie Springs including an assessment of their crystallinity is provided in [46]. The crystallinity (estimated from the infrared splitting factor) of the bones sampled in the current study is reported in the appendix.

Table 1

Samples analysed in the current study: (A) Cuddie Springs, (B) Cretaceous samples. Stratigraphic associations and infrared splitting factor (IRSF) values are provided for samples from Cuddie Springs. IRSF data taken from [46]

Tableau 1

Échantillons analysés dans la présente étude : (A) Cuddie Springs, (B) échantillons crétacés. Les associations stratigraphiques et les valeurs du facteur de dispersion infrarouge (IRSF) sont données pour les échantillons de Cuddie Springs. Les données IRSF proviennent de [46]

A			
Sample code	Stratigraphic		
	Bone	Unit	IRSF
2012	Indet. metatarsal	9	3.03
2014	Indet. fragment	7	3.32
2021	Diprotodon rib	6B	2.99
2024	Genyornis	6B	3.57
2025	Genyornis long bone	6B	3.05
F11 2 D3	Genyornis	7	2.9
F10 27 A13	Indet. fragment	6B	3.09
F11 2 D17	Macropodidae	7	3.71
F10 38 B117	Indet. fragment	9	3.57
F10 38 B118	Indet. fragment	9	3.85
F10 38 C21	Indet. fragment	9	3.79
F10 27 A14	Indet. fragment	6B	nd
F10 19 B161	M. giganteus	6A	3.71
E10 15 D136	Genyornis	6B	3.45
E10 13 A 123	Indet. fragment	6B	3.49
F11 2 A196	Indet. fragment	7	nd
F10 27 A17	Indet. fragment	7	3.07
F10 15 CSB	Macropus sp.		nd
F10 38 C82	Macropodidae	9	3.92
E10 4 A47	Diprotodon		nd

B

Sample code	Bone identification
Dinosaur Park	
DPF 8	Styracosaurus sp. Postorbital
DPF 9	Centrosaurus sp. vertebra fragment
DPF 5	Small theropod metatarsal
DPF 10	Centrosaurus sp. metatarsal
DPF 4	Centrosaurus sp. subadult horn core
DPF 2	Centrosaurus sp. subadult distal radius fragment
DPF 7	Centrosaurus sp. subadult coronoid fragment
DPF 6	Centrosaurus sp. coronoid fragment
DPF 3	Centrosaurus sp. limb bone shaft fragment
DPF 1	Centrosaurus sp. left fibula, partial
DPFOF3	Indet. long bone fragment (mesoreptile)
DPFOF6	Hybodont fin spine
DPFOG8	Indet. long bone fragment (mesoreptile)
DPFOF9	Indet. long bone fragment
Judith River	
BDJR-1	Indet. long bone fragment
BDJR-2	Indet. long bone fragment
BDJR-3	Indet. long bone fragment
BDJR-4	Indet. long bone fragment
BDJR-5	Indet. dense bone fragment
BDJR-6	Indet. flat bone fragment



Table 1 (Continued)

BDJR-7	Indet. rib fragment
BDJR-8	Indet. rib fragment
BDJR-9	Indet. rib fragment
BDJR-10	Indet. fragment
BDJR-11	Indet. fragment
BDJR-12A	Indet. fragment
BDJR-12B	Indet. fragment
BDJR-13	Indet. phalange fragment
BDJR-14	Indet. flat bone fragment
BDJR-15	Indet. phalange fragment
BDJR-16	Indet. distal phalange fragment
BDJR-17	Indet. fragment
BDJR-18	Indet. long bone fragment
Cedar Mountain	
BDCM-1	Uncatalogued turtle bone
BDCM-2	Turtle carapace
BDCM-3	Uncatalogued turtle bone
BDCM-5	Naomichelys shell fragment

## 2.2. Dinosaur Park Formation

13 whole or partial dinosaur bones were obtained from the Late Cretaceous Dinosaur Park Formation (DPF) of Dinosaur Provincial Park, Alberta, Canada. The age of the base of the DPF is constrained by Ar–Ar dates of bentonites to between  $76.43 \pm 0.28$  and  $75.14 \pm 0.16$  Ma [18]. Sediments of the DPF are dominated by fine-medium grained sandstone units deposited within meandering river channels in a coastal plain setting [10,51]. Upper sections of the DPF are increasingly tidally-influenced with the development of extensive mud-filled incised valleys. Bones occur throughout the formation mainly as channel-lag traction-controlled accumulations [9] or as accumulations concentrated on lateral accretion surfaces [10]. All sampled bones are fully recrystallised, light to dark brown in colour and heavily permineralised with calcite, iron oxides and clay minerals. Previous analyses of the REE composition of bones from the Dinosaur Park Formation are provided in [38].

## 2.3. Judith River Formation

Nineteen whole or partial bone samples were obtained from the Late Cretaceous Judith River Formation in central Montana, USA [32]. Fluvial sandstones of the Judith River Formation range from very fine- to medium-grained and are loosely cemented with calcite and clay minerals [32]. Sandstone bodies within the Judith River Formation are interpreted to represent wide, shallow, low sinuosity channels in the lower (regressive) phase and more sinuous, tidally influenced channels in the upper

(transgressive) phase [32]. Fine-grained inter-channel deposits occur throughout the sequence. Carbonaceous claystones indicative of coastal wetland environments are common in the upper transgressive phase. Isolated bones are common throughout the sequence. Bones sampled in this study are indeterminate fragments of long bones, vertebral processes and ribs. All bones are fully recrystallised, light to dark brown and partially to heavily permineralised with calcite, iron oxides and clay minerals.

## 2.4. Cedar Mountain Formation

Four fragments of turtle bone were obtained from the Late Cretaceous Cedar Mountain Formation (CMF) of Utah [4]. The uppermost part of the CMF from which bones were sampled is comprised of variegated mudstones and thin, discontinuous sandstones with bentonitic mudstones and carbonaceous layers [4]. Ar–Ar dates from associated sanidine phenocrysts yield an age of  $98.39 \pm 0.07$  Ma [4]. Bones sampled in this study are fragments of turtle bone or carapace, with one sample attributed to *Naomichelys* sp. Bones are fully recrystallised, black and completely permineralised, principally with calcite.

## 2.5. Analytical methods

The spatial distribution of elements such as U and the REE in bones can be measured relatively easily using modern laser ablation based sampling techniques. Samples from Cuddie Springs were analysed using an ArF (193 nm) Excimer laser (Lambda Physik LPX120i) coupled to an Agilent mass spectrometer housed at the Australian National University Research School of Earth Sciences. Samples from the Judith River, Dinosaur Park and Cedar Mountain Formations were analysed also using an Excimer laser coupled to a PlasmaQuad 2 mass spectrometer at the National Oceanography Centre, Southampton. Prior to analysis, the surface of each sample spot was cleaned by very briefly ablating the exposed bone surface (i.e., to a depth of a few microns). Sample ablation spots approximately 50–70  $\mu\text{m}$  in diameter were selected on the bone sample from the outer surface toward the central bone cortex and inner surface. The depth of sampling spots is estimated at  $\sim 20 \mu\text{m}$ . Sampling locations were manually targeted to avoid cracks and vascular pore spaces. Concentrations of REE and U were measured across each bone section. International glass reference NIST 612 was analysed before and after each bone sample as an external standard.  $^{43}\text{Ca}$  was measured for internal calibration. Average background measurements taken prior to ablation were

subtracted from the measured intensities to calculate sample element concentrations. Sensitivities in the range of 100–20,000 cps/ppm and concentrations less than 1 ppb were detected for the elements tested.

## 2.6. Parameterising concentration profiles

Measured concentration profiles must be parameterised in some way to allow quantitative comparisons between recorded slopes. The diffusion–adsorption (D–A) model [30] potentially provides a powerful method of quantifying rates of element uptake in fossil bone. Unfortunately, distribution coefficients between bone apatite and pore water for the REE are poorly known. The sole experimental determination of apatite–water adsorption coefficients for REE provided estimates from  $\sim 10^6$  to  $10^7$  [21], but these are likely underestimates as equilibrium between apatite and water was probably not achieved in this study. Furthermore, in natural groundwaters, elements such as the REE and U may be bound to a range of ligands, and elemental speciation will profoundly influence both diffusion rates and adsorption coefficients. Finally, the geometry of fossil bones seldom corresponds to the simple slab geometry assumed by the D–A model, with complex variations in the three dimensional distribution of vascular porosity. The combined uncertainties associated with ion speciation, diffusion and adsorption coefficients and sample geometry prevent meaningful estimation of the absolute rate of recrystallisation of bone based on elemental profiles. We therefore provide an alternative approach based simply on parameterising measured concentration gradients by fitting exponential curves using non linear least squares regression rather than estimating the absolute duration of element uptake. This simple method allows comparison of relative rates of recrystallisation between bones and between bone-bearing strata.

The absolute concentration of any element at any point within a fossil bone is partially controlled by the external pore water concentration. To remove the effect of variable pore water concentrations, the concentration of the measured element at any given point is normalised to the concentration at the periosteal surface (the maximum concentration in an ideal concentration gradient) [25]. The measured elemental concentration gradient is then parameterised by fitting an exponential curve with a forced intercept of 1 (Fig. 2). Fossil bones frequently show well-developed concentration profiles for the rare earth elements (REE) but irregular profiles for U. Unlike the REE (excepting Ce and Eu) U is a redox sensitive element, present either as uranyl ( $\text{UO}_4^{2+}$ ) or reduced U complexes. Reduced U is relatively immo-

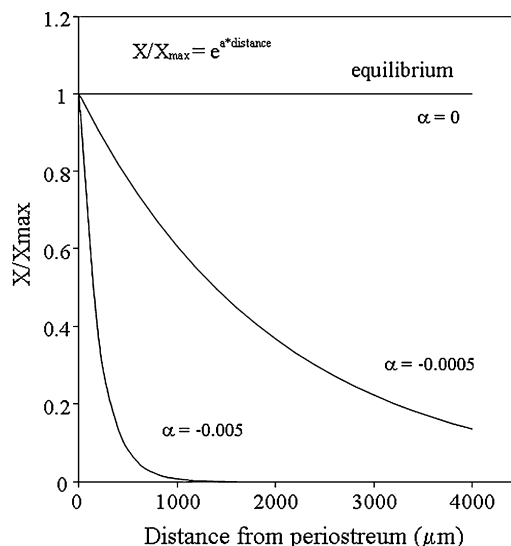


Fig. 2. Parameterisation of measured concentration gradients with simple exponential equations. Increased departure of the exponential from 0 indicates steeper concentration gradients (and potentially more rapid recrystallisation).

Fig. 2. Paramétrisation de gradients de concentration mesurés selon des équations exponentielles simples. L'éloignement accru de l'exponentielle par rapport à zéro indique des gradients de concentration plus pentus (et potentiellement une recrystallisation plus rapide).

bile, thus, the redox conditions present within the bone may influence the distribution of U. Within the REE, lanthanum is present in fossil bones in concentrations that enable accurate and precise measurements by laser ablation ICP–MS. We therefore use elemental profiles of La to compare rates of recrystallisation between bones and between bone bearing strata.

## 3. Results

Measured concentration gradients and fitted exponential curves are provided in Fig. 3. Parameterising variables for measured profiles are provided in Table 2. Of the 60 bones analysed, 41 (68%) yield elemental profiles consistent with single stage uptake by a simple diffusion–adsorption mechanism. All bones from the Cedar Mountain Formation yield gradients consistent with simple D–A uptake. 80% of bones from Cuddie Springs yield D–A type profiles followed by 77% of bones from the Dinosaur Park Formation and 42% of bones from the Judith River Formation.

### 3.1. Cuddie Springs

Of the 20 bones analysed from Cuddie Springs, four failed to yield concentration gradients consistent with

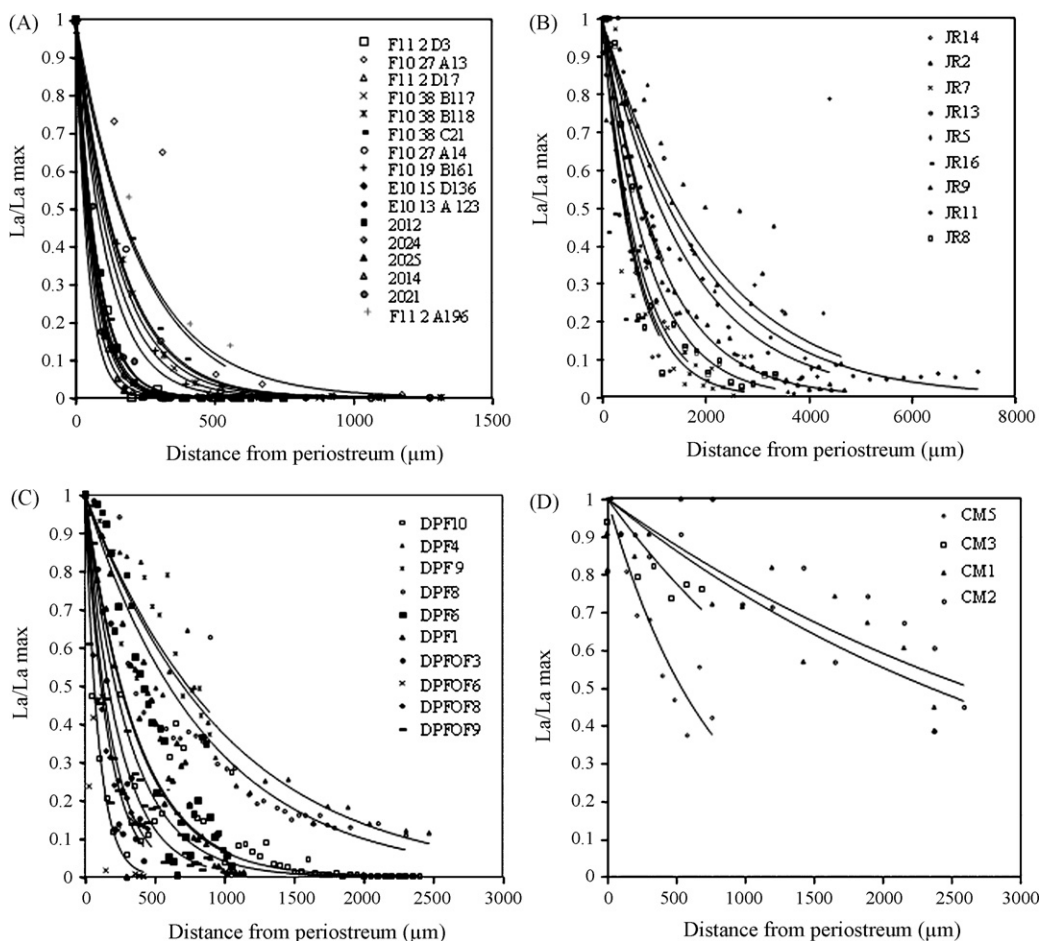


Fig. 3. Measured La concentration gradients and fitted exponential curves from archaeological and fossil bones from (A) Cuddie Springs, (B) Judith River Formation, (C) Dinosaur Park Formation, and (D) Cedar Mountain Formation.

Fig. 3. Gradients de concentration du La mesurés et courbe exponentielle adaptée à partir d'os archéologiques et fossiles provenant (A) de Cuddie Springs, (B) de la formation de Judith River, (C) de la formation de Dinosaur Park et (D) de la formation de Cedar Mountain.

uptake via simple single-phase diffusion–adsorption mechanism. Compared to the other bones from CS, bone F10 15 CSB shows a steep decrease in La concentrations within 100  $\mu\text{m}$  from the periosteal surface and low concentrations of La throughout the remaining thickness of the bone (Fig. 3). The anomalous pattern displayed by this bone may reflect either unusually low La concentrations in surrounding pore waters, or limited bone–water exchange. Assuming that bones from common stratigraphic units within CS experienced similar pore water concentrations, the anomalously steep concentration gradients seen is best explained by limited exchange between bone and pore waters. Bone F10 15 CSB is not fully recrystallised, so pore water exchange cannot have been limited by closure of intra-crystalline porosity. Bone–water exchange must therefore have been

limited by the hydrological conditions immediately surrounding the bone after burial. Bone F10 38 C82 clearly shows leaching of La from the outer surfaces superimposed on a diffusion–adsorption type uptake pattern (Fig. 5A). Two bones (E10 4 A47 and F10 27 A17) display irregular concentration gradients likely reflecting diffusion of REE into the bone from multiple point sources within the cortex (Fig. 5B). The remaining 18 bones analysed from CS yield concentration gradients consistent with uptake via a single phase D–A process. The measured concentration gradients are well approximated with simple exponential relationships (Fig. 3A),  $r^2$  values ranging from 0.69 to 0.97. Best fit curves return exponents ranging from  $-0.0043$  to  $-0.0227$  (Table 2). The mean exponent is  $-0.012$ , with a relative standard deviation of 45%.



Table 2

Curve fit ( $y = e^{\alpha x}$ ) parameters and IRSF values in bones showing simple diffusion–adsorption uptake. IRSF values are taken from Trueman et al. [46]

Table 2

Paramètres ( $y = e^{\alpha x}$ ) et valeurs d'IRSF dans des os montrant un enrichissement par simple adsorption–diffusion. Valeurs d'IRSF tirées de Trueman et al. [46]

Bone	$\alpha$	$r^2$
Cuddie Springs		
F11 2 D3	−0.0156	0.77
F10 15 CSB	−0.0067	0.73
F10 27 A13	−0.0043	0.92
F10 38 C82	−0.0089	0.88
F11 2 D17	−0.0135	0.69
F10 38 B117	−0.0089	0.98
F10 38 B118	−0.0063	0.89
F10 38 C21	−0.0067	0.92
F10 27 A14	−0.0061	0.93
F10 19 B161	−0.0076	0.94
E10 15 D136	−0.0146	0.86
E10 13 A 123	−0.0187	0.97
2012	−0.0132	0.83
2024	−0.0154	0.89
2025	−0.0166	0.91
2014	−0.0227	0.97
2021	−0.0131	0.86
F11 2 A196	−0.0041	0.69
Dinosaur Park		
DPF10	−0.0026	0.86
DPF4	−0.001	0.92
DPF9	−0.0009	0.68
DPF8	−0.0011	0.84
DPF6	−0.0013	0.53
DPF1	−0.0018	0.55
DPFOF3	−0.0035	0.78
DPFOF6	−0.0063	0.4
DPFOF8	−0.0032	0.91
DPFOF9	−0.0024	0.77
Judith River		
JR14	−0.0014	0.58
JR2	−0.0009	0.96
JR7	−0.0016	0.74
JR13	−0.0009	0.27
JR5	−0.0007	0.55
JR9	−0.0005	0.77
JR11	−0.0005	0.79
JR8	−0.0011	0.79
Cedar Mountain		
CM5	−0.0013	0.77
CM3	−0.0005	0.29
CM1	−0.0003	0.65
CM2	−0.0003	0.61

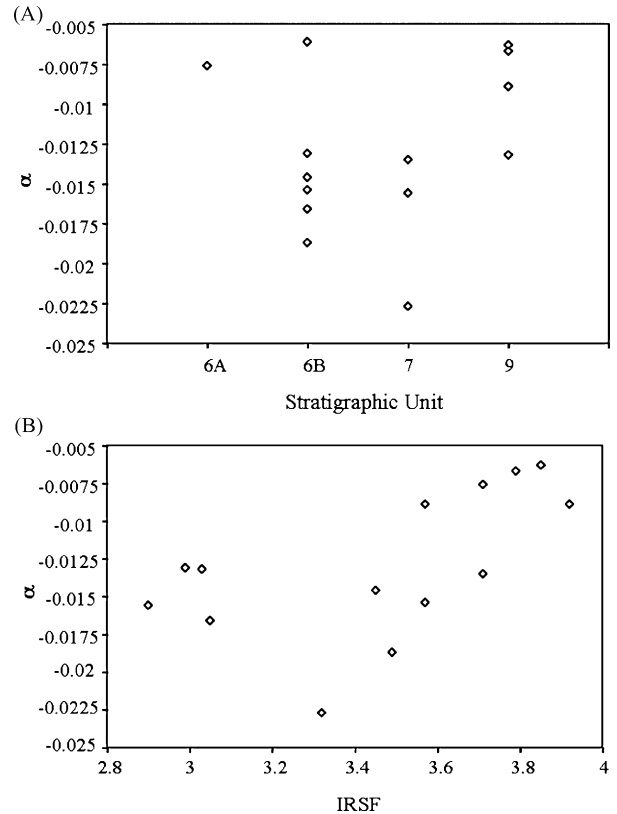


Fig. 4. Relationship between fitted exponent ( $\alpha$ ) and (A) Stratigraphic Unit and (B) infrared splitting factor in bones from Cuddie Springs.

Fig. 4. Relation entre l'exposant  $\alpha$  adapté et l'unité stratigraphique (A) et le facteur de dispersion infrarouge (B) dans des os de Cuddie Springs.

### 3.2. Dinosaur Park Formation

Of the 13 bones analysed from the Dinosaur Park Formation, three failed to yield concentration gradients consistent with uptake via simple single-phase diffusion–adsorption mechanism (Fig. 6). DPF 5 shows a profile characterized by high concentrations in the outermost regions falling sharply to relatively low and uniform concentrations (Fig. 6A). This profile may represent late diagenetic uptake at the outer margins of a bone with a pre-existing uptake history (with further penetration limited by the lack of pore space in recrystallised bone), extremely rapid recrystallisation or limited access to REE-containing pore waters. La concentrations in the interior cortex of bone DPF 5 exceed 100 ppm, indicating that significant uptake occurred throughout the cortex prior to enhanced uptake at the outer margins (Fig. 6A). The distribution of La in the cortex of bone DPF 2 shows high, uniform concentrations in the outermost 2 mm, followed by a reduction in La concentrations

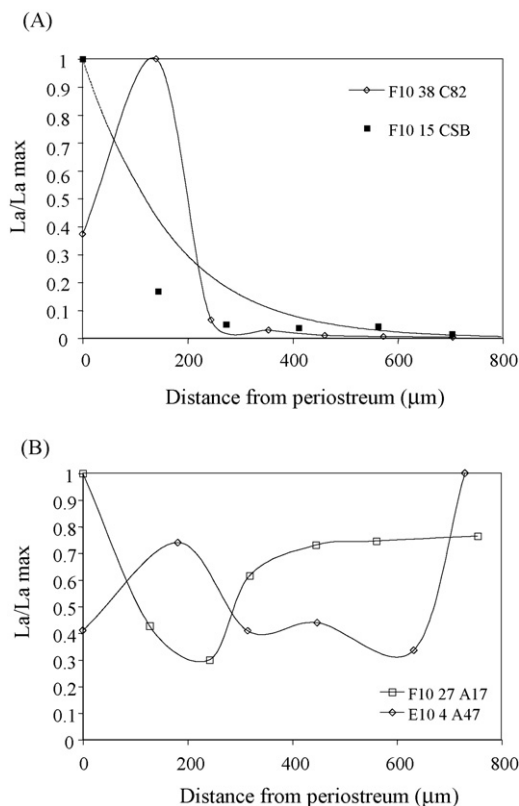


Fig. 5. Measured La concentration profiles in bones from Cuddie Springs that do not conform to simple diffusion–adsorption uptake. (A) Leached and oversteepened concentration gradients, (B) irregular concentration gradients.

Fig. 5. Gradients de concentration de La, mesurés dans des os de Cuddie Springs qui ne se comportent pas selon un modèle d'enrichissement par simple diffusion–adsorption. (A) Gradients de concentration par lessivage. (B) Gradients de concentration irréguliers.

consistent with uptake via D–A (Fig. 6B). This pattern suggests relatively rapid delivery of La within the outer cortex, possibly through vascular channels, with further internal diffusion of La limited by differences in vascular architecture. Bone DPFOF1 shows extremely low concentrations of REE at the outer margin with distinct peaks in REE occurring within the cortex (Fig. 6C). This profile is difficult to explain, but may reflect either strong leaching of REE or distribution of REE tightly controlled by patterns of fluid flow within the cortex, themselves governed by histology. The remaining 10 bones analysed from DPF yield concentration gradients consistent with uptake via a single phase D–A process. Fitted exponential curves give  $r^2$  values ranging from 0.40 to 0.92 with exponents ranging from  $-0.0009$  to  $-0.0105$  (Table 2). The mean exponent is  $-0.0024$ , with a relative standard deviation of 68%.

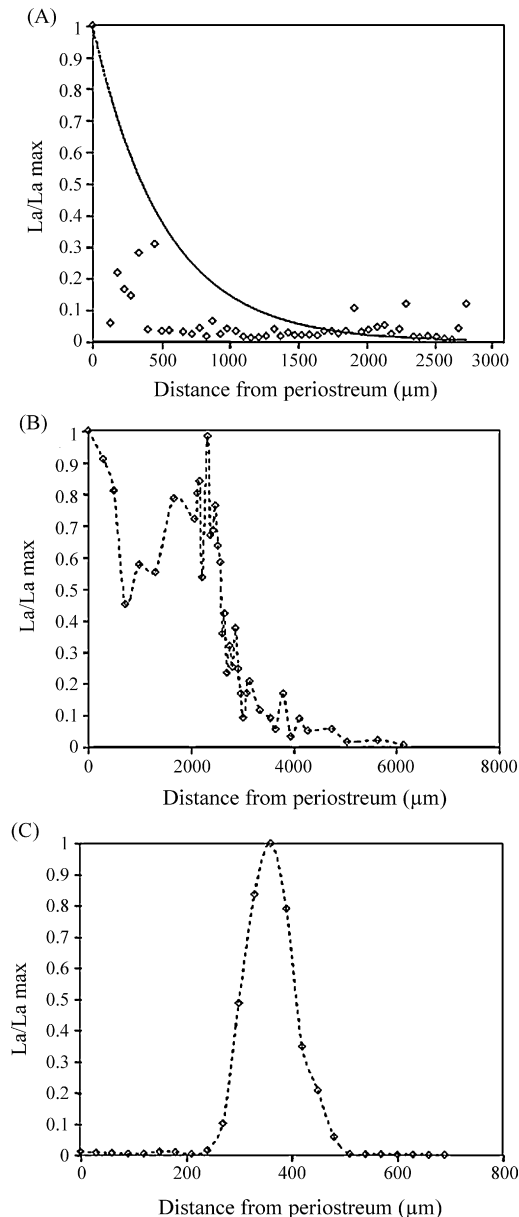


Fig. 6. Measured La concentration gradients and best fit exponential curves from bones from the Dinosaur Park Formation that do not show gradients consistent with simple diffusion–adsorption uptake. (A) Measured profile is too steep to fit an exponential curve – an 'oversteepened' gradient, (B) two-phase diffusion adsorption gradient, (C) leached, and/or complex uptake profile.

Fig. 6. Gradients mesurés de concentration de La et meilleures courbes exponentielles adaptées pour des os de la formation Dinosaur Park qui ne présentent pas de gradients, en accord avec un modèle d'enrichissement par simple diffusion–adsorption. (A) Profil mesuré trop pentu pour s'accorder à une courbe exponentielle – c'est un gradient en « surpente ». (B) Gradient d'adsorption–diffusion biphasique. (C) Profil de lessivage et/ou d'enrichissement complexe.

### 3.3. Cedar Mountain Formation

All four bones analysed from the Cedar Mountain Formation yield concentration gradients consistent with uptake via simple single-phase diffusion–adsorption mechanism (Fig. 3). Fitted exponential curves give  $r^2$  values ranging from 0.29 to 0.77 with exponents ranging from  $-0.0003$  to  $-0.0013$  (Table 2). The mean exponent is  $-0.0006$ , with a relative standard deviation of 79%.

### 3.4. Judith River Formation

Of the 19 bones analysed from the Judith River Formation, 11 failed to yield a concentration gradient consistent with uptake via simple single-phase diffusion–adsorption mechanisms, the highest proportion of all four sites. Profiles inconsistent with single-phase D–A uptake fall into one or more of three

categories, high-edge profiles, leached profiles, and irregular profiles (Fig. 7). Bone JR17 shows a profile similar to DPF5, with high concentrations in the outermost regions falling sharply to relatively low and uniform concentrations (Fig. 7A). La concentrations in the interior cortex of bone JR17 exceed 100 ppm, suggesting that this profile represents late diagenetic uptake at the outer margins of a bone with a pre-existing uptake history with further penetration limited by the lack of pore space in recrystallised bone. Bones JR14, JR12 and JR10 show clear evidence of leaching of La at outer margins (Fig. 7B). Irregular profiles (Fig. 7C) are shown by eight bones. Irregular distribution of La is most likely caused by complex diffusion patterns, ions diffusing from multiple sources within vascularised bone. The remaining eight bones analysed from the JRF yield concentration gradients consistent with uptake via a single phase D–A process. Fitted exponential curves give  $r^2$  values ranging

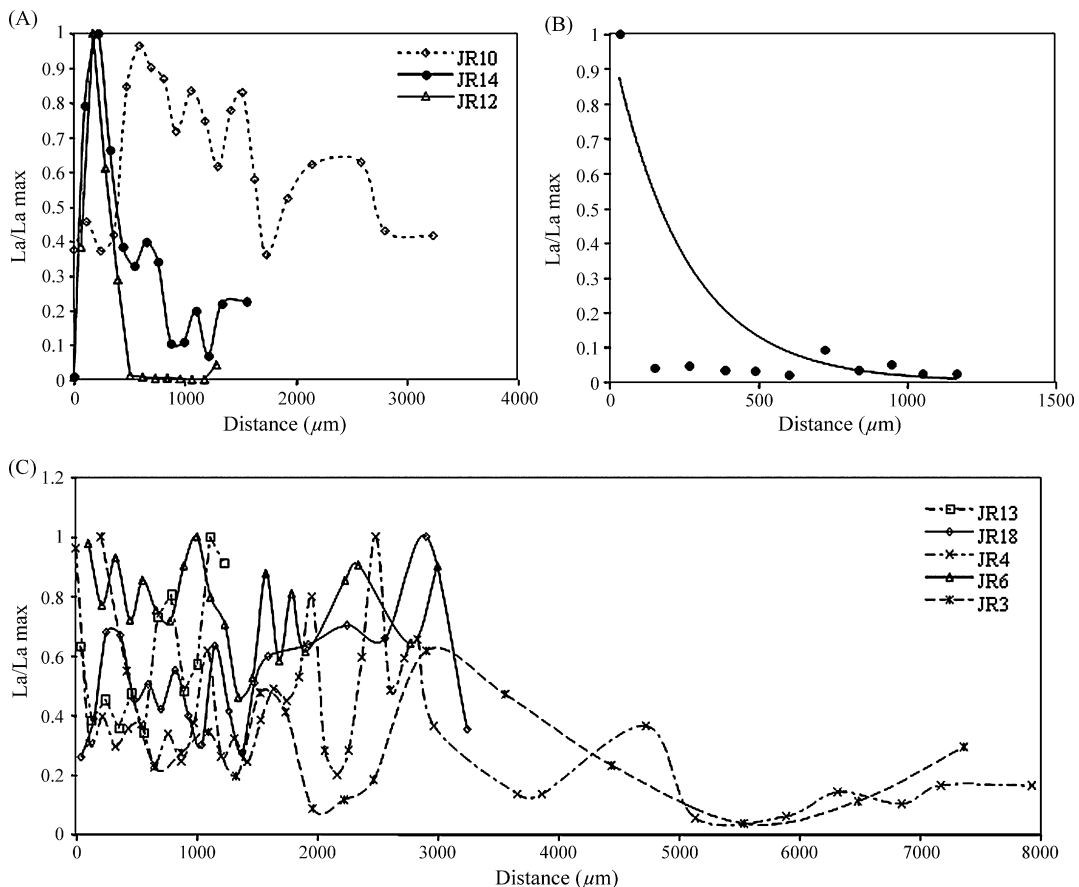


Fig. 7. Measured La concentration gradients and best fit exponential curves from bones from the Judith River Formation that do not show gradients consistent with simple diffusion–adsorption uptake. (A) Leached gradients, (B) oversteepened gradients, (C) some examples of irregular gradients. Fig. 7. Gradients mesurés de concentration en La et meilleure courbe exponentielle adaptée pour des os de la formation Judith River qui ne présentent pas de gradients en accord avec un modèle d'enrichissement par simple diffusion–adsorption. (A) Gradients de lessivage. (B) Gradients trop pentus. (C) Quelques exemples de gradients irréguliers.

from 0.16 to 0.96 with exponents ranging from  $-0.0005$  to  $-0.0016$  (Table 2). The mean exponent is  $-0.0010$ , with a relative standard deviation of 42%.

## 4. Discussion

### 4.1. Development of concentration gradients in archaeological bones

The concentration gradients developed in bones from Cuddie Springs show no clear relationship with stratigraphic level (Fig. 4A), suggesting that, although many bones from Cuddie Springs are not fully recrystallised, La uptake has not been continuous since deposition, and probably occurred soon after burial [44]. There is no strong relationship between concentration gradients and crystallinity in the entire Cuddie Springs dataset (Fig. 4B). If bones showing no appreciable recrystallisation ( $\text{IRSF} < 3.2$  [46]) are excluded, however, then there is a significant positive relationship between crystallinity and concentration gradient ( $r^2 = 0.71$ ,  $P = 0.002$ ), with more recrystallised bones displaying shallower concentration gradients. This is counter-intuitive as enhanced recrystallisation might be expected to reduce porosity and therefore, reduce uptake of trace elements. Both recrystallisation and trace element uptake require interaction between bone and groundwater, therefore, the relationship between these two variables suggests that both recrystallisation and trace element uptake were limited by access to pore waters. In all bones from Cuddie Springs the REE appear to have incorporated rapidly while REE-containing pore waters were in contact with the bones. During the period of pore water exposure some bones achieved complete recrystallisation. Those bones that did not fully recrystallise during this time presumably have a reduced probability of ultimate survival into deep time. After the period of pore water exposure, the chemical data indicate that no further uptake of REE occurred in either recrystallised or unrecrystallised bones.

### 4.2. Relative rates of recrystallisation: variation within sites

Bones from the Judith River Formation show the widest range in uptake styles, strongly suggesting that these bones experienced a high degree of variation in depositional microenvironments, and that the microenvironment of burial significantly affected the nature of bone–water interaction during diagenesis. The potential for preservation of either geochemical or molecular information in bones from the Judith River Formation

is also likely to vary extensively with as yet unknown aspects of depositional microenvironment.

Rates of recrystallisation of bone are also expected to vary with hydrological conditions. This is demonstrated by the ranges in measured concentration gradients observed within each of the sampled fossil sites. Bones from the Dinosaur Park and Cedar Mountain formations show high relative standard deviations around the mean exponential fit, indicating a wide range in recrystallisation rates compared with bones from the Judith River Formation and Cuddie Springs site. These results could be interpreted to reflect the range of depositional microenvironments that are conducive to recrystallisation and long-term preservation in each of these sites. A narrow range in concentration gradients could imply that specific hydrological conditions are necessary for recrystallisation to occur, and that unless these precise conditions are met, bones will not survive. On the contrary, a wide range in developed concentration gradients might suggest less dependence on specific hydrological conditions to achieve recrystallisation, and thus greater overall preservation potential for bone. Where a range of concentration gradients exists, bones with the steepest, smooth concentration gradients (indicative of relatively rapid recrystallisation that may effectively ‘seal in’ biochemical information) are more likely to yield intact biomolecules or biogenic chemical data.

### 4.3. Relative rates of recrystallisation: variation between sites

The mean concentration gradient returned for any one locality or assemblage provides a measure of the mean extent of bone–pore water interaction, which in most palaeontological cases will reflect the mean rate of recrystallisation. Steep concentration gradients imply less interaction between bone and pore waters due either to rapid recrystallisation or to restricted recharging of pore waters. In the sampled sites, the mean concentration gradient in the archaeological bones from Cuddie Springs is significantly steeper site than in any of the three Cretaceous sites (Table 3), and the total REE concentrations in bones from Cuddie Springs are also significantly lower than those from the Cretaceous sites. This implies that bones from Cuddie Springs experienced significantly less bone–water interaction and/or faster rates of recrystallisation than those from the other three sites. While bones from Cuddie Springs do not retain sufficient collagen for stable isotope analyses or  $^{14}\text{C}$  dating, recrystallised bones from Cuddie Springs are potentially good candidates for the recovery of biomolecular fossils due to their fast recrystallisation rates.

Within the Cretaceous samples, the mean concentration gradient in bones from the Dinosaur Park Formation is significantly steeper than that from the Judith River or Cedar Mountain Formations suggesting faster rates of recrystallisation (or less bone–water interaction), and greater potential for recovery of intact molecular or geochemical information. It should be noted, however, that bones from the Dinosaur Park Formation also display a wide range in concentration gradients. Thus, while the Dinosaur Park Formation as a whole appears to be the most conducive formation for preservation of intact biogeochemical information, the likelihood of such preservation varies significantly between bones.

Bones from the Cedar Mountain Formation yield the shallowest gradients of all bones measured, suggesting that the extent of bone–water interaction and/or time taken to achieve recrystallisation was relatively large at this site, and that bones from Cedar Mountain Formation are relatively unlikely to yield pristine molecular or geochemical data.

## 5. Conclusions

The significance of this approach is that relative rates of fossilisation of any bones can be determined analytically. This allows an assessment of the sedimentological, environmental and hydrographic conditions controlling recrystallisation rates in bone. The conceptual model of bone diagenesis proposed suggests that long-term preservation of organic macromolecules may occur where recrystallisation rates are particularly fast. Measurement of trace element concentration profiles offers a method to test this suggestion and, if true, provides a technique to prospect for localities or bones from which intact biomolecules or geochemical information may be recovered. The hypotheses presented above are preliminary, but highlight the potential taphonomic information contained in the distribution of trace elements within fossil bones. Future challenges involve testing the relationship between trace element distributions and taphonomic state.

## Acknowledgements

The authors thank Steve Eggins at ANU and Andy Milton at NOCS for assistance with laser ablation ICP–MS analyses.

## References

- [1] J.M. Asara, M.H. Schweitzer, L.M. Freimark, M. Phillips, L.C. Cantley, Protein sequences from *Mastodon* and *Tyrannosaurus rex* revealed by mass spectrometry, *Science* 316 (2007) 280–285.
- [2] F. Berna, A. Matthews, S. Weiner, Solubilities of bone mineral from archaeological sites: the recrystallisation window, *J. Archaeol. Sci.* 31 (2004) 867–882.
- [3] H. Bocherens, A. Tresset, F. Weidemann, F. Giligny, F. Lafage, Y. Lanchon, A. Mariotti, Diagenetic evolution of mammal bone in two French Neolithic sites, *Bull. Soc. geol. France* 168 (1997) 555–564.
- [4] R.L. Cifelli, J.I. Kirkland, A. Weil, A.L. Deino, B.J. Kowallis, High-precision  $^{40}\text{Ar}/^{39}\text{Ar}$  geochronology and the advent of North America's Late Cretaceous terrestrial fauna, *Proc. Natl. Acad. Sci. USA* 94 (1997) 11163–11167.
- [5] M.J. Collins, M.S. Riley, A.M. Child, G. Turner-Walker, A basic mathematical simulation of the chemical degradation of ancient collagen, *J. Archaeol. Sci.* 22 (1995) 175–183.
- [6] M.J. Collins, A.M. Gernaey, C.M. Nielsen-Marsh, C. Vermeer, P. Westbroek, Slow rates of degradation of osteocalc: green light for fossil bone protein? *Geology* 28 (2000) 1139–1142.
- [7] M.J. Collins, C.M. Nielsen-Marsh, J. Hiller, C.I. Smith, J.P. Roberts, R.V. Prigodich, et al., The survival of organic matter in bone: a review, *Archaeometry* 44 (2002) 383–394.
- [8] J. Coltrain, J. Field, R. Cosgrove, J. O'Connell, Stable isotope and protein analyses of Cuddie Springs Genyornis, *Archaeol. Oceania* 39 (2004) 50–51.
- [9] D.A. Eberth, Stratigraphy and sedimentology of vertebrate microfossil localities in uppermost Judith River Formation (Campanian) of Dinosaur Provincial Park, *Palaeogeogr. Palaeoclimatol. Palaeoecol.* 78 (1990) 1–36.
- [10] D.A. Eberth, A.P. Hamblin, Tectonic, stratigraphic and sedimentologic significance of a regional discontinuity in the upper Judith River Group (Belly River wedge) of southern Alberta, Saskatchewan, and northern Montana, *Can. J. Earth Sci.* 30 (1993) 174–200.
- [11] T.A. Elliott, G.W. Grime, Examining the diagenetic alteration of human bone material from a range of archaeological burial sites using nuclear microscopy, *Nucl. Instrum. Phys. Res. B* 77 (1993) 537–547.
- [12] J.C. Elliott, Calcium Phosphate Biominerals, in: M.J. Kohn, J. Rakovan, J.M. Hughes, (Eds.), *Phosphates: geochemical, geological and materials importance*, Mineral. Soc. Am. Rev. Mineral. Geochem. 48 (2002), 426–453.
- [13] J. Field, R. Fullagar, G. Lord, A large area archaeological excavation at Cuddie Springs, *Antiquity* 75 (2001) 696–702.
- [14] P. Grandjean, H. Cappelletta, A. Michard, F. Albarède, The assessment of REE patterns and  $^{143}\text{Nd}/^{144}\text{Nd}$  ratios in fish remains, *Earth Planet Sci. Lett.* 84 (1987) 181–196.
- [15] R.E.M. Hedges, A.R. Millard, Bones and groundwater: towards the modelling of diagenetic processes, *J. Archaeol. Sci.* 22 (2) (1995) 155–164.
- [16] J.F. Hubert, P.T. Panish, D.J. Chure, K.S. Prostak, Chemistry, microstructure, petrology and diagenetic model of Jurassic dinosaur bones, Dinosaur National Monument, Utah, *J. Sediment Res.* 66 (1996) 531–547.
- [17] J.F. Humpala, P.H. Ostrom, H. Gandhi, J.R. Strahler, A.K. Walker, T.W. Stafford Jr., et al., Investigation of the protein osteocalcin of *Camelops hesternus*: sequence, structure and phylogenetic implications, *Geochim. Cosmochim. Acta* 71 (2007) 5956–5967.
- [18] K. Janssens, L. Vincze, B. Vekemans, C.T. Williams, M. Radtke, M. Haller, et al., The non-destructive determination of REE in fossilized bone using synchrotron radiation induced K-line X-ray microfluorescence analysis, *Fresenius' J. Anal. Chem.* 363 (1999) 413–420.



- [19] L.S. Keto, S.B. Jacobsen, Nd and Sr isotopic variations of Early Paleozoic oceans, *Earth Planet. Sci. Lett.* 84 (1987) 27–41.
- [20] L. Kocsis, T.W. Vennemann, D. Fontigne, Migration of sharks into freshwater systems during the Miocene and implications for Alpine Paleoelevation, *Geology* 35 (2007) 451–454.
- [21] D. Koeppenastrop, E.H. Decarlo, Sorption of rare-earth elements from seawater onto synthetic mineral particles – an experimental approach, *Chem. Geol.* 95 (1992) 251–263.
- [22] M.J. Kohn, J.M. Law, Stable isotope composition of fossil bone as a new paleoclimate indicator, *Geochim. Cosmochim. Acta* 70 (2006) 931–946.
- [23] B.J. MacFadden, J. Labs-Hochstein, R.C. Hulbert Jr., J.A. Bas-kin, Revised age of the late Neogene terror bird (*Titanis*) in North America during the Great American interchange, *Geology* 35 (2007) 123–126.
- [24] E.E. Martin, B.A. Haley, Fossil fish teeth as proxies for seawater Sr and Nd isotopes, *Geochim. Cosmochim. Acta* 64 (2000) 835–847.
- [25] A.R. Millard, R.E.M. Hedges, A diffusion–adsorption model of uranium uptake by archaeological bone, *Geochim. Cosmochim. Acta* 60 (1999) 2139–2152.
- [26] J. Moradian-Oldak, S. Weiner, L. Addadi, W.J. Landis, W. Traub, Electron imaging and diffraction study of individual crystals of bone, mineralized tendon and synthetic carbonate apatite, *Connect. Tissue Res.* 25 (1991) 219–228.
- [27] B.K. Nelson, M.J. DeNiro, M.J. Schoeninger, D.J. DePaolo, P.E. Hare, Effects of diagenesis on strontium, carbon, nitrogen and oxygen concentration and isotopic composition of bone, *Geochim. Cosmochim. Acta* 50 (1986) 1941–1949.
- [28] C.M. Nielsen-Marsh, R.E.M. Hedges, Patterns of diagenesis in bone I: the effects of site environments, *J. Archaeol. Sci.* 27 (2000) 1139–1150.
- [29] C.M. Nielsen-Marsh, P.H. Ostrom, H. Gandhi, B. Shapiro, A. Cooper, P.V. Hauschka, et al., Sequence preservation of osteocalcin protein and mitochondrial DNA in bison bones older than 55 ka, *Geology* 30 (2002) 1099–1102.
- [30] A.W.G. Pike, R.E.M. Hedges, P. van Calstreen, U-series dating of bone using the diffusion–adsorption model, *Geochim. Cosmochim. Acta* 66 (2002) 4273–4286.
- [31] S.J. Roberts, C.I. Smith, A. Millard, M.J. Collins, The taphonomy of cooked bone: characterizing boiling and its physico-chemical effects, *Archaeometry* 44 (2002) 485–494.
- [32] R.R. Rogers, Sequence analysis of the Upper Cretaceous two medicine and Judith River Formations, Montana: nonmarine response to the Clagget and Bearpaw marine cycles, *J. Sediment Res.* 68 (1988) 615–631.
- [33] M.A. Rubin, I. Jasiuk, J. Taylor, J. Rubin, T. Ganey, R.P. Apkarian, TEM analysis of the nanostructure of normal and osteoporotic human trabecular bone, *Bone* 33 (2003) 270–282.
- [34] M.H. Schweitzer, J.L. Wittmeyer, J.R. Horner, Soft tissue and cellular preservation in vertebrate skeletal elements from the Cretaceous to the present, *Proc. R. Soc. Lond. B Biol. Sci.* 274 (2007) 183–197.
- [35] A. Sillen, J.E. Parkington, Diagenesis of bone from Elands Bay Cave, *J. Archaeol. Sci.* 23 (1996) 535–542.
- [36] C.I. Smith, O.C. Craig, R.V. Prigodich, C.M. Nielsen-Marsh, M.M.E. Jans, C. Vermeer, et al., Diagenesis and survival of osteocalcin in archaeological bone, *J. Archaeol. Sci.* 32 (2005) 105–113.
- [37] R. Staron, B. Grandstaff, W. Gallagher, D.E. Grandstaff, REE signals in vertebrate fossils from Sewel, NJ: implications for location for the K–T boundary, *Palaio* 16 (2001) 255–265.
- [38] C.N. Trueman, Rare earth element geochemistry and taphonomy of terrestrial vertebrate assemblages, *Palaio* 14 (1999) 446–459.
- [39] C.N. Trueman, M.J. Benton, A geochemical method to trace the taphonomic history of reworked bones in sedimentary settings, *Geology* 25 (1997) 263–266.
- [40] C.N. Trueman, D.M. Martill, The long-term preservation of bone: the role of bioerosion, *Archaeometry* 44 (2002) 371–382.
- [41] C.N. Trueman, N. Tuross, Trace elements in recent and fossil bone, in: M.J. Kohn, J. Rakovan, J.M. Hughes, (Eds.), *Phosphates: geochemical, geobiological and materials importance*, Mineral. Soc. Am. Rev. Mineral. Geochem. 48 (2002), 489–521.
- [42] C. Trueman, C. Chenery, D.A. Eberth, B. Spiro, Diagenetic effects on the oxygen isotope composition of bones of dinosaurs and other vertebrates recovered from terrestrial and marine sediments, *J. Geol. Soc. Lond.* 160 (2003) 1–7.
- [43] C.N.G. Trueman, A.K. Behrensmeyer, N. Tuross, S. Weiner, Mineralogical and compositional changes in bones exposed on soil surfaces in Amboseli National Park, Kenya: diagenetic mechanisms and the role of sediment pore fluids, *J. Archaeol. Sci.* 31 (2004) 721–739.
- [44] C.N. Trueman, J.H. Field, J. Dortch, B. Charles, S. Wroe, Prolonged coexistence of humans and megafauna in Pleistocene Australia, *Proc. Natl. Acad. Sci. USA* 102 (2005) 8383–8385.
- [45] C.N. Trueman, A.K. Behrensmeyer, R. Potts, N. Tuross, High-resolution records of location and relative age from the rare earth element composition of fossil bones, *Geochim. Cosmochim. Acta* 70 (2006) 4343–4355.
- [46] C.N. Trueman, K. Privat, J.F. Field, Why do crystallinity values fail to predict the extent of diagenetic alteration of bone mineral?, *Palaeogeogr. Palaeoclimatol. Palaeoecol.* (in press).
- [47] S. Weiner, P.A. Price, Disaggregation of bone into crystals, *Calcif. Tissue Int.* 39 (1986) 365–375.
- [48] S. Weiner, W. Traub, Organization of hydroxyapatite crystals within collagen fibrils, *FEBS Lett.* 206 (1986) 262–266.
- [49] C.T. Williams, Element distribution maps in fossil bones, *Archaeometry* 30 (1988) 237–247.
- [50] C.T. Williams, P. Henderson, C.A. Marlow, T.I. Molleson, The environment of deposition indicated by the distribution of rare earth elements in fossil bones from Olduvai Gorge, Tanzania, *Appl. Geochem.* 12 (1997) 537–547.
- [51] J.M. Wood, R.G. Thomas, J. Visser, Fluvial processes and vertebrate taphonomy: the Upper Cretaceous Judith River Formation, South Central Dinosaur Provincial Park, Alberta, Canada, *Palaeogeogr. Palaeoclimatol. Palaeoecol.* 66 (1998) 127–143.
- [52] J. Wright, R.S. Seymour, H.F. Shaw, REE and Nd isotopes in conodont apatite: variations with geological age and depositional environment, in: D.L. Clark (Ed.), *Conodont Bio-facies and Provincialism*, Geol. Soc. Am. Spec. Pap., (1984), 325–340.
- [53] T.G. Zocco, H.L. Schwarcz, Microstructural analysis of bone of the sauropod dinosaur *Seismosaurus* by transmission electron microscopy, *Palaeontology* 37 (1994) 493–503.